REACTIVE FLOW MODELING OF THE INTERACTION OF TATB DETONATION WAVES WITH INERT MATERIALS*

Craig M. Tarver and Estella M. McGuire
Lawrence Livermore National Laboratory
Livermore, CA 94551

The Ignition & Growth model for the shock initiation and detonation of solid explosives is applied to calculating the main features of detonation waves in the triaminotrinitrobenzene (TATB) based high explosives LX-17, PBX 9502 and EDC-35. Under detonation conditions, TATB based explosives exhibit reaction zone lengths of 2 to 3 mm depending on the interactions between the detonation wave and the surrounding inert materials. This paper describes comparisons of Ignition & Growth calculations with data from several two- and three-dimensional experiments in which various materials are used to confine the TATB based explosives. The calculated unconfined failure diameters of PBX 9502 are normalized to the measured values at five initial temperatures. Failure diameters for LX-17 are then estimated by changing only the fraction ignited near the shock front. Fabry-Perot data on spherically divergent LX-17 "snowball" experiments is also compared to calculations. Calculated detonation velocities, wave front curvatures, and metal acceleration velocities are compared to experimental detonation data for TATB-based high explosives in tantalum, copper, PMMA, brass, and beryllium confinement. Three-dimensional prism failure test results on PBX 9502 are also stimulated using the ALE3D code.

INTRODUCTION

Triaminotrinitrobenzene (TATB) - based solid explosives are widely used due to their excellent safety characteristics. Three high density versions are: LX-17 (92.5% TATB/7.5% KelF); PBX 9502 (95% TATB/5% KelF); and EDC-35 (95% TATB/5% KelF). These explosives exhibit 2 to 3 mm reaction zone lengths and many non-ideal propagation properties when detonating.[1] The Ignition & Growth reactive flow model has been applied to a great deal of experimental data on TATB detonation waves in order to predict this non-ideal behavior in geometries that can not be tested. Numerous one-dimensional embedded gauge and laser interferometer experiments on detonating LX-17 and PBX 9502 have created an excellent database for reactive flow modeling.[2] Various two-dimensional experiments have shed considerable light on the detonation versus charge diameter, failure diameter, and wave curvature properties of detonating TATB.[3] The three-dimensional prism failure test[4] has also provided an excellent test for TATB reactive flow modeling. In this paper, several of the most interesting two-and three-dimensional experiments on these three TATB-based explosives are described and calculated. The results are used to determine the ability of the model to predict a wide range of confinement effects ranging from no confinement (failure diameter cylindrical rate sticks and spherical divergence) to medium confinement (PMMA and beryllium cylinders) to heavy confinement (brass, steel, copper, and tantalum cylinders).

THE IGNITION & GROWTH MODEL

The Ignition and Growth reactive flow model of shock initiation and detonation of solid explosives has been used to solve many 1D, 2D, and 3D explosive and propellant safety and performance problems.[5-11] The model uses two Jones-Wilkins-Lee (JWL) equations of state, one for the unreacted explosive and one for its reaction products, in the temperature dependent form:

$$p = A\,e^{-R_1 V} + B\,e^{-R_2 V} + \omega C_V T/V \qquad (1)$$

where p is pressure in Megabars, V is relative volume, T is temperature, ω is the Gruneisen coefficient, C_V is the average heat capacity, and A, B, R_1, and R_2 are constants. The reaction rate law for the conversion of explosive to products is:

$$dF/dt = I(1-F)^b(\rho/\rho_0-1-a)^x + G_1(1-F)^cF^dp^y$$
$$(0<F<F_{igmax}) \qquad (0<F<F_{G1max})$$
$$+ G_2(1-F)^eF^gp^z \qquad (2)$$
$$(F_{G2min}<F<1)$$

where F is the fraction reacted, t is time, ρ is the current density, ρ_0 is the initial density, and I, G_1, G_2, a, b, c, d, e, g, x, y, and z are constants. The mixture equations assume pressure and temperature equilibration between the unreacted explosive and its reaction products.

This three-term rate law describes the three stages of reaction generally observed in shock initiation and detonation of heterogeneous solid explosives. For detonation, the first term represents the ignition of the explosive as it is compressed by the leading shock wave creating heated areas (hot spots) as the voids in the material collapse. The fraction of explosive ignited is approximately equal to the original void volume.[5] The second reaction models the rapid formation of the major reaction product gases (CO_2, N_2, H_2O, CO, etc.) in highly vibrationally excited states[12] and their subsequent expansion and equilibration. The third term is used to describe the relatively slow diffusion controlled formation of the solid carbon particles in the form of diamond, graphite, or amorphous carbon. For TATB-based explosives, the last 20% of the energy release is assumed to be solid carbon formation. Other LX-17 and Ultrafine TATB Ignition and Growth applications are shown in companion papers.[13,14] The mesh sizes used in these calculations are 10 and 20 zones per mm. The results are independent of mesh size so the modeling has converged to consistent answers.

FAILURE DIAMETER RESULTS

The failure diameter of PBX 9502 has been determined at five initial temperatures: -55˚C; 24˚C; 75˚C, 170˚C and 250˚C. For the first three temperatures, the conventional cylindrical rate stick measurements of Campbell[15,16] are used. For the highest two temperatures, the prism test results of Asay and McAfee[17] are used.

An Ignition & Growth reactive flow model for PBX 9502 based on the widely used LX-17 model was developed for the shock initiation embedded gauge experiments of Gustavsen et al.[18] The only changes were to decrease the critical compression [parameter a in Eq. (2)] at which reaction begins from 0.22 for LX-17 to 0.214 for PBX 9502 and to increase the maximum fraction reacted ignited by the first term of Eq. (2) from 0.02 for LX-17 to 0.025 for PBX 9502 {Figmax in Eq. (2)}. These two changes are based on the experimental facts that PBX 9502 reacts at slightly lower shock pressures than LX-17 and that PBX 9502 is typically pressed to 97.5% of its theoretical maximum density (TMD), while LX-17 is pressed to 98% TMD. Table 1 contains all of the Ignition & Growth equation of state and reaction rate parameters used for LX-17 and PBX 9502. The calculated failure diameters of PBX 9502 at these five initial temperatures were then normalized to the experimental values by varying G_1 and the pressure exponent y in the second (reaction growth) term of Eq. (2). Growth coefficients G_1 were obtained for both y=2 and y=3, both of which have been used to model TATB-based reaction rates in previous work.

In unconfined failure diameter calculations, the use of y=3 yields relatively fast failure of detonation after a few centimeters of propagation at the limiting experimental detonation velocities (7.4 mm/μs for PBX 9502).[16] The use of y=2 also yields failure at the correct diameters and velocities, but this failure process requires long distances (20 to 40 cm) of propagation. Experimentally, Campbell[16] has demonstrated that the failure of a PBX 9502 detonation wave in a cylindrical rate stick can take 25 to 30 cm. Therefore using y=2 in Eq. (2) is more physically correct, but using y=3 yields sharp failure/detonation limits at much shorter run distances. The two pressure dependencies give essentially the same results for all of the experiments discussed in this paper. Table 2 lists the values of G_1 and y used for each initial temperature of PBX 9502, the experimental failure diameter or twice the failure thickness, and calculated failure/detonation diameter. These calculated values predict failure diameter to within 1 mm, and more exact values could be determined.

The failure diameter of LX-17 has never been determined, but it is assumed to be midway between the 95% TATB/ 5% KelF and 90% TATB/ 10% KelF values of Campbell and Engelke.[15] Table 2 contains the calculated failure diameters for LX-17 at –55˚C, 24˚C, and 75˚C determined by changing only parameters "a" and Figmax in Eq. (2). Recent work on ambient temperature LX-17 has shown that its failure diameter is very close to the calculated estimate of 11 – 12 mm.[13] It is encouraging that the ignition term of the model is sensitive enough to predict a change in failure diameter of 7 – 8 mm for PBX 9502 to 11 – 12 mm for LX-17 by just accounting for the differences in porosity. Ignition & Growth predicts the increase in failure diameter as the initial density approaches TMD for LX-17, a well-known phenomenon for carbon rich explosives like TATB and TNT,[19] but more experimentation at higher densities and large diameters is required.[13] Experiments to determine the failure diameter of LX-17 at –55˚C and 75˚C are planned to check the predicted failure diameters listed in Table 2.

DIVERGING LX-17 DETONATION WAVES

In a companion paper, Druce et al.[14] present Fabry-Perot velocity history measurements at 5 angles for spherically diverging detonation waves in LX-10 and Ultrafine TATB booster explosives and the corresponding Ignition and Growth reactive flow calculations of the entire experimental geometries. Fabry-Perot experiments have also been fired in which 1.15 cm shells of LX-17 have placed between the Ultrafine TATB boosters and the PMMA windows. These "snowball tests" measure the breakout times and interface particle velocity histories at 7˚, 30˚, 60˚, 75˚, and 85˚. Figure 1 shows the experimental Fabry-Perot records for three LX-17 snowball tests and the Ignition & Growth calculations using the LX-17 parameters in Table 1 and the Ultrafine TATB, aluminum, steel, LX-16, PBX 9407, and PMMA parameters given by Druce et al.[13] The calculated arrival times are in the correct order (60˚, 30˚, 75˚, 7˚, and finally 85˚), and the calculated maximum interface particle velocities for LX-17 impacting PMMA agree well with experiment. These particle velocities have not reached the C-J values for LX-17, thereby indicating

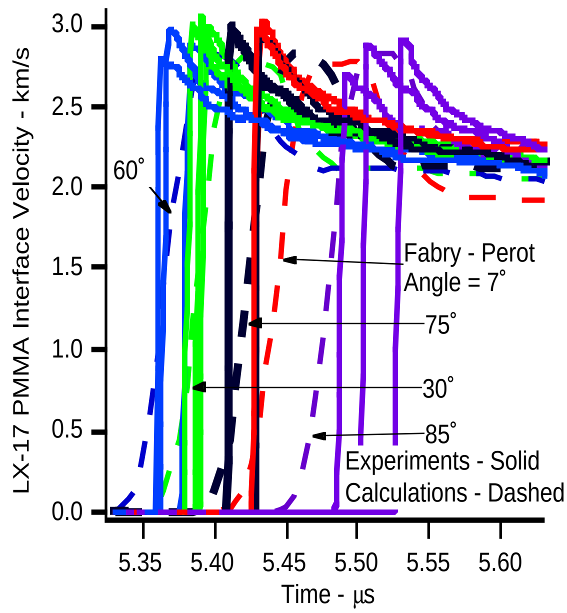

FIGURE 1. EXPERIMENTAL AND CALCULATED INTERFACE PARTICLE VELOCITY HISTORIES FOR LX-17 SNOWBALLS AND PMMA WINDOWS

that the LX-17 detonation wave is still growing toward its steady state strength. These results agree closely with a previous study by Bahl et al.[7] Spherical divergence is one of the most difficult and most important geometries for reactive flow models to predict, and the agreement shown in Fig. 1 is excellent proof of the accuracy of the LX-17 detonation model in that geometry.

CONFINED CYLINDRICAL LX-17 WAVES

LX-17 cylinders have been fired using copper, tantalum, and PMMA tubes. Streak cameras and Fabry-Perot laser interferometry are used to measure the wall velocity histories. Detonation wave curvature measurements were made on the top of the LX-17 charges in the case of copper and PMMA. Several copper cylinder tests were fired using 2.5417 cm radius LX-17 cylinders confined by 0.2721 cm thick copper tubes. The Fabry-Perot records for one of these shots showed evidence of spall in the copper tube, while those from the other shots did not. The experiments were modeled using the LX-17 parameters shown in Table 1 and the Steinberg-Guinan model[20] with the Gruneisen parameters listed in Table 3. The spall strength was set equal to –1.8 GPa, as determined for high explosive driven spall in copper discs by Tarver and Maiden.[21] A second calculation was done with the spall option turned off. Figure 2 shows the Fabry-Perot record and the Ignition & Growth simulation with the spall model off for a copper cylinder test that did not spall, while Fig. 3 shows similar records with the spall model on for the cylinder that did spall. Both calculations agree very well with the tests, except for the initial jump-off velocity. The streak cameras and Fabry-Perot laser interferometers do not resolve this initial velocity well, because of the air shock wave and the early time angle variations of the copper motion. The Fabry-Perot lasers are set at 7˚ for copper. Ignition & Growth modeling shows that the maximum velocity vector settles down to 7˚ before the second shock jump but varies significantly at earlier times.

A close examination of the calculated pressure states in the copper walls indicated that the spall criterion is reached only periodically in the wall. So the Fabry-Perot and streak cameras will only record spall-like patterns when they are focused on an area of high tension. Only one of three LX-17/Cu cylinder tests with these dimensions spalled. Spall was only predicted by using both the Ignition & Growth and the Steinberg-Guinan models.

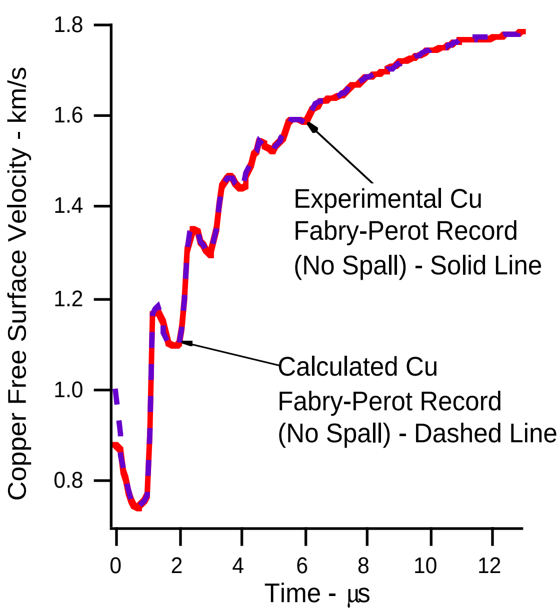

FIGURE 2. LX-17 COPPER CYLINDER TEST RESULTS WITHOUT SPALL

One tantalum cylinder was fired using LX-17 about 10 years ago.[22] The LX-17 radius was 2.5415 cm and the Ta thickness was 0.2717 cm. Figure 4 shows the Ta cylinder Fabry-Perot record and the corresponding Ignition & Growth modeling results.

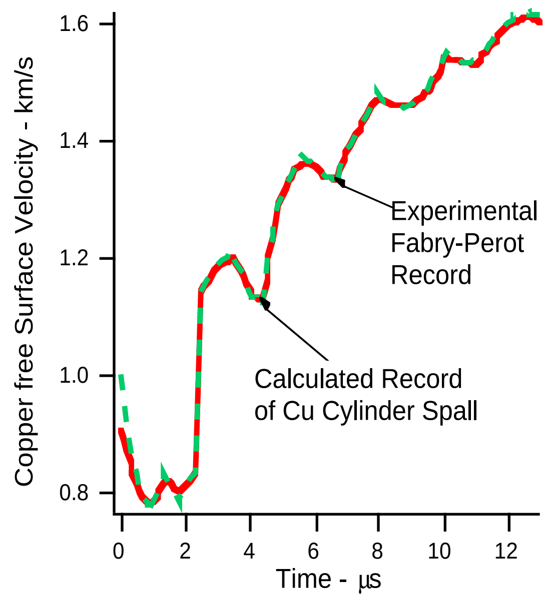

FIGURE 3. LX-17 COPPER CYLINDER TEST RESULTS WITH SPALL

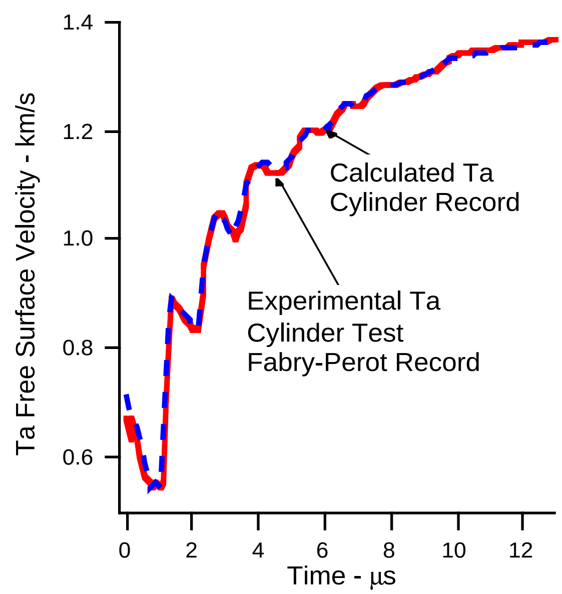

FIGURE 4. LX-17 TANTALUM CYLINDER TEST RESULTS (NO SPALL OBSERVED)

The Fabry-Perot angle was set at 5˚ as determined by Ignition & Growth modeling. The agreement is excellent except for the initial jump-off velocity. No evidence of Ta spall was observed experimentally or computationally using a –8.0 GPa criteria for high explosive driven Ta spall.[21]

Recently some LX-17 cylinders were detonated using PMMA confining tubes.[23] The LX-17 radius was 1.27 cm and the PMMA was also 1.27 cm thick. A very thin layer of aluminum was placed on the inner wall of the PMMA cylinder so the Fabry-Perot would record the interface velocity history of the reaction products and the PMMA. Unfortunately, the Fabry-Perot angle was mistakenly set at 7˚, while both analytical theory[24] and Ignition & Growth calculations showed that the angle should have been set at approximately 35˚. Since the cosine of 7˚ is 0.9925, the Fabry-Perot velocimeters essentially measured the radial component of the interface velocity. In Fig. 5, the average of 9 Fabry-Perot records and the calculated radial velocity for the interface between detonating LX-17 and PMMA are compared for the 0.8 µs that the longest experimental records lasted.

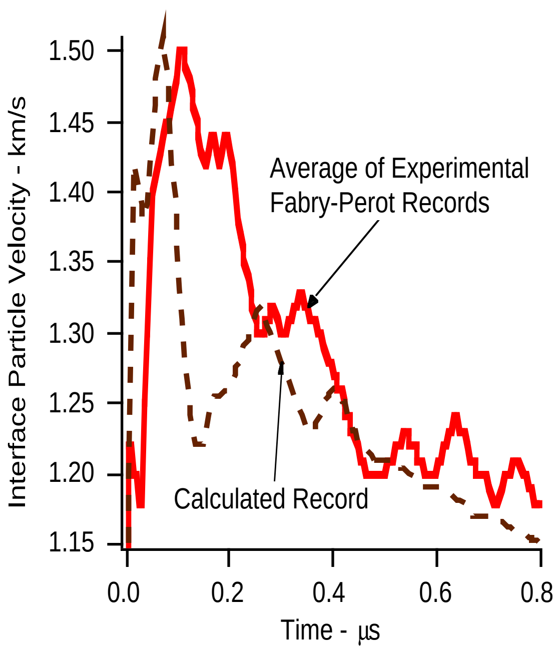

FIGURE 5. INTERFACE PARTICLE VELOCITY HISTORIES FOR LX-17 PMMA RADIAL CYLINDER TEST EXPANSION

The wave curvature at the top of the LX-17 charges was measured for two copper cylinders and a PMMA cylinder. Unfortunately, curvature was not measured for the tantalum cylinder test. Figure 6 contains two experimental wave curvatures for copper and one PMMA and the calculated curvatures for copper, PMMA, and tantalum confinement. Combining this data with that for unconfined LX-17 and LX-17 confined by teflon shown in a companion paper,[13] the LX-17 reactive flow model's calculated wave curvatures are very close to experiment for a wide range of confinement strengths. Thus the LX-17 model yields excellent descriptions of the curved detonation wave front and inert material acceleration in cylindrical geometry.

THE INTERACTION OF EDC35 WAVES WITH BRASS AND BERYLLIUM WALLS

Eden and Belcher[25] reported an excellent study of the effects of brass and beryllium walls on the propagation velocity of detonating 25 mm thick slabs of EDC35. The EDC35 slabs were initiated by 25 mm square cross section Composition B boosters. The brass plates were 10 mm thick, while the beryllium plates were 9.3 mm thick. The arrival times were measured at 20, 40, 60, 80, and

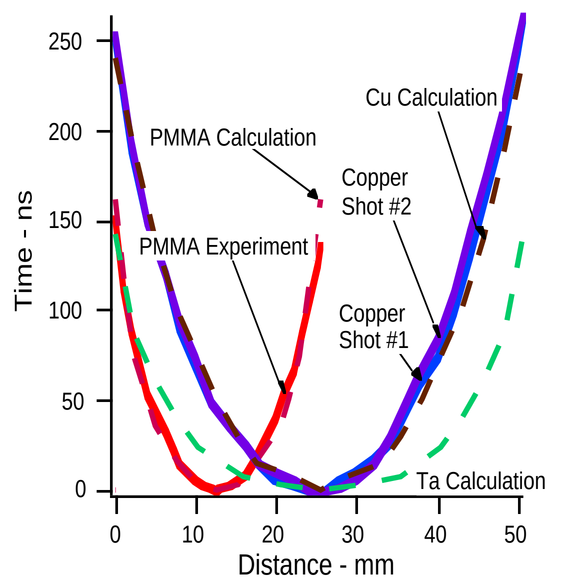

FIGURE 6. LX-17 DETONATION WAVE CURVATURE FOR PMMA, COPPER, AND TANTALUM CYLINDERS

100 mm of EDC35 detonation wave propagation along the beryllium interface and at the corresponding positions in the brass. Like copper, tantalum, and PMMA, brass has a lower shock velocity than the EDC35 detonation velocity, and normal curved front patterns like those in Fig. 6 are observed. However, beryllium has a higher shock velocity than the EDC 35 detonation velocity and therefore "pulls" the detonation wave along at higher than normal detonation velocities at the EDC35-Be interface. An Ignition & Growth calculation was done of the entire experiment using the PBX 9502 parameters in Table 1 for EDC35, a C-J detonation model for Composition B shown in Table 4, and the brass and beryllium parameters shown in Table 3. This calculation reproduced all of the effects observed experimentally: an elastic wave in Be traveling at over 12 km/s; a slower propagation of the EDC35 wave along the brass surface; a faster propagation along the Be surface; and even a weak shock moving at about 3 km/s with about 3 GPa pressure connecting the EDC35 wave to the Be shock front. Table 5 shows the comparisons of the experimental and calculated arrival time differences at the 5 measurement distances and the average propagation velocities of the EDC35 detonation wave along the two inert surfaces. The agreement between the Ignition & Growth predictions and the experimental results is excellent. The model predicts slightly faster propagation along the Be than observed experimentally and thus slightly greater timing differences between the brass and Be arrival times. Figure 7 shows the EDC35 detonation wave pressure contours at 18.676 μs at breakout of the leading detonation front after 100 mm of propagation with the leading Be shock on the right side and the lagging brass shock front on the left. This snapshot is very similar to the experimental records of Eden and Belcher.[25] Thus the model did an excellent job of simulating the effect of the Be wall on the propagation of an EDC35 detonation.

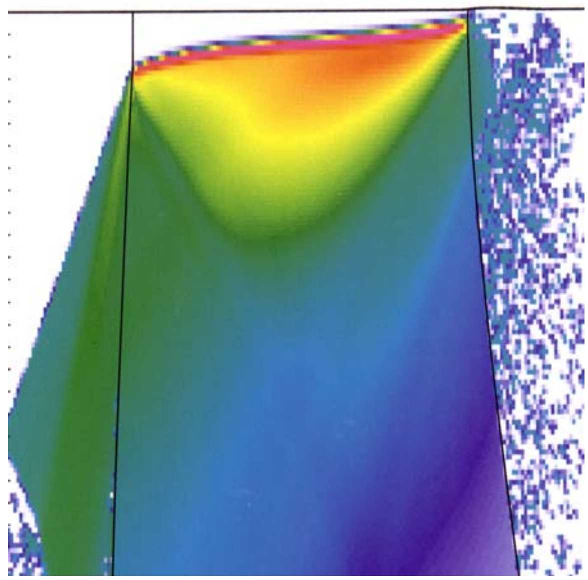

FIGURE 7. PRESSURE CONTOURS FOR AN EDC-35 DETONATION WAVE AFTER 100 MM OF PROPAGATION ALONG A BRASS WALL (LEFT SIDE) AND A BERYLLIUM WALL (RIGHT SIDE)

THREE-DIMENSIONAL PRISM FAILURE TEST MODELING FOR PBX 9502

The three-dimensional prism test for detonation failure developed by Ramsay[4] is an excellent test of the PBX 9502 reactive flow parameters. In this test, a detonation wave is initiated with a 150 mm long line-wave generator into a 12 x 12 x 150 mm booster of PBX 9501 (95wt% HMX/ 5%estane-plasticizer binder). This detonation wave travels into a 12 x 12 x 150 mm booster of PBX 9502 and then into a 150 mm long, 50 mm wide wedge of PBX 9502 with a 2˚ taper. The base of the wedge was 8 mm thick and the toe 2 mm thick for most shots. The thickness at the point of detonation failure is measured from the dent formed in a dural witness plate. An experiment using two PBX 9502 prisms edge-to-edge provided a total run distance of 100 mm and showed that the prism failure thickness is very close to 1/2 of the cylindrical rate stick failure diameter. Various inert materials were used to confine the PBX 9502 prisms and reduce the failure thicknesses.[4] Asay and McAfee[17] used the prism test to estimate the failure diameter of PBX 9502 heated to 170˚C and 250˚C. All of the other experiments modeled in this paper have an axis of symmetry and can be modeled as two-dimensional in the DYNA2D, LS-DYNA2D, and CALE codes. This prism test is truly three-dimensional and must be modeled as such. Three-dimensional meshes of the entire prism test were developed for the LS-DYNA3D and ALE3D codes, which contain identical versions of the Ignition & Growth model.

The 3D reactive flow modeling of the prism test shows that the whole prism face begins to react when hit by the PBX 9502 donor detonation wave. However, this reaction begins to fail almost immediately at the narrow edge of the wedge. The failure of reaction moves inward faster for reaction growth rates that depend upon pressure cubed than for those which depend on pressure squared. This failure of reaction continues until a wedge thickness of approximately 4 mm is reached after 2 to 3 cm of propagation. The PBX 9502 detonation then propagates with small oscillations until the end of 5 cm long wedge is reached. Therefore the calculated failure thickness of unconfined PBX 9502 is very close to the experimental value of 4 mm, which is approximately half of the cylindrical failure diameter. The calculated effects of confinement density and thickness on the prism failure thickness will be compared to experimental measurements of Ramsay[4] in a later paper.

CONCLUSIONS

The LX-17 and PBX 9502 detonation Ignition & Growth reactive flow models were shown to accurately simulate a wide variety of two- and three-dimensional experiments, which used confinements ranging from none to very heavy. They can be used with confidence to predict 2D and 3D detonation propagation in scenarios which can not be tested. More sophisticated reactive flow models are being developed,[26] but the accuracy and reliability of the Ignition & Growth model in several 2D and 3D hydrodynamic codes will continue to make it a very useful tool for shock initiation and detonation modeling and predictions for the foreseeable future.

ACKNOWLEDGEMENTS

The authors would like to thank Robert Druce and David Goosman for their Fabry-Perot records, David Aldis for the tantalum cylinder test report, and Albert Nichols for many helpful discussions concerning the ALE3D code.

*This work was performed under the auspices of the United States Department of Energy by the University of California, Lawrence Livermore National Laboratory under Contract No. W-7405-ENG-48.

REFERENCES

1. Dobratz, B. M., “The Insensitive High Explosive TATB: Development and Characterization – 1888 to 1994,” Los Alamos National Laboratory Report LA-13014-H, UC-741, August 1995.

2. Tarver, C. M., Kury, J. W., and Breithaupt, R. D., “Detonation Waves in Triaminotrinitrobenzene,” J. Appl. Phys. **82**, 3771 (1997).

3. Tarver, C. M. and Hallquist, J. O., “Modeling Two-Dimensional Shock Initiation and Detonation Wave Phenomena in PBX 9404 and LX-17,” Seventh Symposium (International) on Detonation, NSWC MP 82-334, Annapolis, MD, 1981, p. 488.

4. Ramsay, J. B., “Effect of Confinement on Failure in 95 TATB/5 KEL-F,” Eighth Symposium (International) on Detonation, Naval Surface Weapons Center NSWC 86-194, Albuquerque, NM, 1985, p. 372.

5. Tarver, C. M., Hallquist, J. O., and Erickson, L. M., “Modeling Short Pulse Duration Shock Initiation of Solid Explosives,” Eighth Symposium (International) on Detonation, Naval Surface Weapons Center NSWC 86-194, Albuquerque, NM, 1985, p. 951.

6. Urtiew, P. A., Erickson, L. M., Aldis, D. F., and Tarver, C. M., “Shock Initiation of LX-17 as a Function of its Initial Temperature,” Ninth Symposium (International) on Detonation, Office of the Chief of Naval Research OCNR 113291-7, Portland, OR, 1989, p. 112.

7. Bahl, K., Bloom, G., Erickson, L., Lee, R., Tarver, C., Von Holle, W., and Weingart, R., “Initiation Studies on LX-17 Explosive,” Eighth Symposium (International) on Detonation, Naval Surface Weapons Center NSWC MP 86-194, Albuquerque, NM, 1985, p. 1045.

8. Urtiew, P. A., Cook, T. M., Maienschein, J. L., and Tarver, C. M., “Shock Sensitivity of IHE at Elevated Temperatures,” Tenth International Detonation Symposium, Office of Naval Research, ONR 33395-12, Boston, MA, 1993, p. 139.

9. Urtiew, P. A., Tarver, C. M., Maienschein, J. L., and Tao, W. C., "Effect of Confinement and Thermal Cycling on the Shock Initiation of LX-17," Combustion and Flame **105**, 43 (1996).

10. Tarver, C. M., "Modeling Shock Initiation and Detonation Divergence Test on TATB-Based Explosives," Propellants, Explosives and Pyrotechnics **15**, 132 (1990).

11. Urtiew, P.A., Tarver, C. M., Forbes, J. W., and Garcia, F., "Shock Sensitivity of LX-04 at Elevated Temperatures," Shock Compression of Condensed Matter-1997, S. C. Schmidt, D. P. Dandekar, J. W. Forbes, eds., AIP Conference Proceedings 429, Woodbury, NY, 1998, p. 727.

12. Tarver, C. M., "Multiple Roles of Highly Vibrationally Excited Molecules in the Reaction Zones of Detonation Waves," J. Phys. Chem. **101**, 4845 (1997).

13. Tran, T., Tarver, C., Maienschein, J., Lewis, P., Moss, M., Druce, R., Lee, R., and Roeske, F., "Characterization of Detonation Wave Propagation in LX-17 near the Critical Diameter," paper presented at this Symposium.

14. Druce, R., Roeske, F., Fried, L., Souers, P. C., Tarver, C., Chow, C., Lee, R., McGuire, E., Overturf, G., Haskins, J., Schneberk, P., and Vitello, P., "Propagation of Axially Symmetric Detonation Waves," paper presented at this Symposium.

15. Campbell, A. W. and Engelke, R., "The Diameter Effect in High-Density Heterogeneous Explosives," Sixth Symposium (International) on Detonation, Office of Naval Research ACR-221, Coronado, CA, 1976, p. 642.

16. Campbell, A. W., "Diameter Effect and Failure Diameter of a TATB-Based Explosive," Propellants, Explosives, Pyrotechnics **9**, 183 (1984).

17. Asay, B. W. and McAfee, J. M., "Temperature Effects on Failure Thickness and DDT in PBX 9502 and TATB," Tenth International Detonation Symposium, Office of Naval Research, ONR 33395-12, Boston, MA, 1993, p. 485.

18. Gustavsen, R. L., Sheffield, S. A., Alcon, R. R., Forbes, J. W., Tarver, C. M., and Garcia, F., "Embedded Electromagnetic Gauge Measurements and Modeling of Shock Initiation in the TATB-Based Explosives PBX 9502 and LX-17," Shock Compression of Condensed Matter-2001, M. D. Furnish, N. N. Thadhani, and Y. Horie, eds., CP-620, AIP Press, 2002, p. 1019.

19. Price, D., "The Detonation Velocity – Loading Density Relation for Selected Explosives and Mixtures of Explosives," J. Energetic Materials **1**, 55 (1983).

20. Steinberg, D. J. and Guinan, M. W., "A High-Strain Rate Constititive Model for Metals," Lawrence Livermore National Laboratory Report No. UCRL-80465 (1978).

21. Tarver, C. M. and Maiden, D. E., "Experimental Measurements and Numerical Simulations of Metal Spallation by Detonating High Explosives," Shock Waves in Condensed Matter – 1987, S. C. Schmidt, N. C. Holmes, eds., Elsevier Science B. V., 1988, p. 363.

22. Aldis, D. F., Quirk, W., and Breithaupt, R. D., "The Effect of Detonation Curvature on Cylindrical Wall Motion," Lawrence Livermore National Laboratory Report UCRL-ID-107480, May 1991.

23. Goosman, D. R., Lawrence Livermore National Laboratory, Private Communication, 2001.

24. Neal, T., "Perpendicular Explosive Drive and Oblique Shocks," Sixth Symposium (International) on Detonation, Office of Naval Research ACR-221, Coronado, CA, 1976, p. 602.

25. Eden, G. and Belcher, R. A., "The Effects of Inert Walls on the Velocity of Detonation in EDC35, An Insensitive High Explosive," Ninth Symposium (International) on Detonation, Office of the Chief of Naval Research OCNR 113291-7, Portland, OR, 1989, p. 831.

26. Nichols, A. L. III and Tarver, C. M., "A Statistical Hot Spot Reactive Flow Model for Shock Initiation and Detonation of Solid High Explosives," paper presented at this Symposium.

TABLE 1. IGNITION & GROWTH PARAMETERS FOR LX-17, PBX 9502 AND EDC35

A. 25 °C LX-17 ρ_o =1.905 g/cm^3

UNREACTED JWL	PRODUCT JWL	REACTION RATES	
A=632.07 Mbar	A=14.8105 Mbar	I=4.0x10^6 μs^{-1}	
B= -0.04472 Mbar	B=0.6379 Mbar	a=0.22	
R_1=11.3	R_1=6.2	b=0.667	
R_2=1.13	R_2=2.2	x=7.0	F_{igmax}=0.02
ω=0.8938	ω=0.5	G_1=1100 Mbar$^{-2}\mu s^{-1}$	
C_V=2.487x10^{-5} Mbar/K	C_V=1.0x10^{-5} Mbar/K	c=0.667	
T_o = 298°K	E_O=0.069 Mbar	d=1.0	
Shear Modulus=0.0354 Mbar		y=2.0	F_{G1max}=0.8
Yield Strength=0.002 Mbar		G_2=30 Mbar$^{-1}\mu s^{-1}$	
		e=0.667	z=1.0
		g=0.667	FG2min=0.8

B. 25°C PBX 9502 ρ_o =1.895 g/cm^3

UNREACTED JWL	PRODUCT JWL	REACTION RATES	
A=632.07 Mbar	A=13.6177 Mbar	I=4.0x10^6 μs^{-1}	
B= -0.04472 Mbar	B=0.7199 Mbar	a=0.214	
R_1=11.3	R_1=6.2	b=0.667	
R_2=1.13	R_2=2.2	x=7.0	F_{igmax}=0.025
ω=0.8938	ω=0.5	G_1=1100 Mbar$^{-2}\mu s^{-1}$	
C_V=2.487x10^{-5} Mbar/K	C_V=1.0x10^{-5} Mbar/K	c=0.667	
T_o = 298°K	E_O=0.069 Mbar	d=1.0	
Shear Modulus=0.0354 Mbar		y=2.0	F_{G1max}=0.8
Yield Strength=0.002 Mbar		G_2=30 Mbar$^{-1}\mu s^{-1}$	
		e=0.667	z=1.0
		g=0.667	F_{G2min}=0.8

C. –54°C PBX 9502 and LX-17 ρ_o = 1.895 g/cm^3

T_O = 219°K B = -0.03928 Mbar G_1 = 900 Mbar^{-2} μs^{-1} G_2 = 30 Mbar$^{-1}\mu s^{-1}$

D. 75°C PBX 9502 and LX-17 ρ_o = 1.895 g/cm^3

To = 348°K B = -0.048162 Mbar G1 = 1500 Mbar$^{-2}\mu s^{-1}$ G2 = 30 Mbar$^{-1}\mu s^{-1}$

E. 170°C PBX 9502 ρ_o = 1.895 g/cm^3

To = 443 °K B = -0.0547 Mbar G1 = 2000 Mbar$^{-2}\mu s^{-1}$ G2 = 30 Mbar$^{-1}\mu s^{-1}$

F. 250°K PBX 9502 ρ_o = 1.895 g/cm^3

To = 523°K B = -0.060206 Mbar G1 = 2400 Mbar$^{-2}\mu s^{-1}$ G2 = 30 Mbar$^{-1}\mu s^{-1}$

G. EDC35 To = 298°K ρ_o = 1.900 g/cm3 Other parameters – same as PBX 9502

TABLE 2. EXPERIMENTAL & CALCULATED FAILURE DIAMETERS FOR PBX 9502 AND LX-17

		FAILURE DIAMETER (mm)		GROWTH COEFFICIENTS	
EXPLOSIVE	To (˚K)	Experimental	Calculated	G_1(y=2)(Mbars$^{-2}\mu s^{-1}$)	G_1(y=3)(Mbars$^{-3}\mu s^{-1}$)
PBX 9502	298	>7 & <8	>7 & <8	1100	4200
PBX 9502	348	>5 & <6	>5 & <6	1500	7200
PBX 9502	219	>10 & <11	>10 & <11	900	3750
PBX 9502	443	>4 & <5**	>4 & <5	2000	7500
PBX 9502	523	>3 & <4**	>3 & <4	2400	8000
LX-17	298	~ 12	>11 & <12	1100	4200
LX-17	348		>8 & <9	1500	7200
LX-17	219		>15 & <16	900	3750

** Twice the failure thickness measured in the LANL Prism Test[4,17]

TABLE 3. GRUNEISEN EQUATION OF STATE PARAMETERS FOR INERT MATERIALS

$$P = \rho_o c^2 \mu[1+(1-\gamma_o/2)\mu - a/2\mu^2]/[1-(S_1-1)\mu - S_2\mu^2/(\mu+1) - S_3\mu^3/(\mu+1)^2]^2 + (\gamma_o + a\mu)E,$$

where $\mu = (\rho/\rho_o - 1)$ and E is thermal energy

INERT	ρ_o(g/cm^3)	c(mm/µs)	S_1	S_2	S_3	γ_o	a
Al 6061	2.703	5.24	1.4	0.0	0.0	1.97	0.48
Steel	7.90	4.57	1.49	0.0	0.0	1.93	0.5
PMMA	1.186	2.57	1.54	0.0	0.0	0.85	0.0
Brass	8.45	3.834	1.43	0.0	0.0	2.0	0.0
Beryllium	1.85	8.0	1.124	0.0	0.0	1.11	0.16
Copper	8.93	3.94	1.489	0.0	0.0	2.02	0.47

TABLE 4. JONES – WILKINS – LEE (JWL) PARAMETERS FOR C-J DETONATION

A. LX-16 (96% PETN, 4% FPC 461) ρ_o = 1.7g/cm^3; D = 0.7963 cm/µs; P_{CJ} = 0.30507 Mbars;
A = 5.16784 Mbars; B = 0.24491 Mbars; R_1 = 4.5; R_2 = 1.5; ω = 0.29; Eo = 0.0986 Mbar-cc/cc-g

B. PBX 9407 (94% RDX, 6% Exon 461) ρ_o = 1.6 g/cm^3; D = 0.7910 cm/ms; P_{CJ} = 0.265 Mbars;
A = 5.73187 Mbars; B = 0.14639 Mbars; R_1 = 4.6; R_2 = 1.4; ω = 0.32; Eo =0.086 Mbar-cc/cc-g

C. Composition B ρ_o = 1.717 g/cm^3; D = 0.798 cm/µs; P_{CJ} = 0.295 Mbars;
A = 5.242 Mbars; B = 0.07678 Mbars; R_1 = 4.2; R_2 = 1.1; ω = 0.34; Eo = 0.085 Mbar-cc/cc-g

TABLE 5. COMPARISON OF DETONATION VELOCITIES AND ARRIVAL TIMES FOR EDC35 ALONG BRASS AND BERYLLIUM SLABS

Distance along Wall (mm)	Differences in Arrival Times: Experimental(µs)	Calculated (µs)
0	0	0
20	0.059	0.076
40	0.142	0.164
60	0.186	0.213
80	0.215	0.251
100	0.223	0.300

Average Detonation	Experimental: Brass	Beryllium	Calculated: Brass	Beryllium
Velocities (mm/µs)	7.63 – 7.69	7.77 – 7.83	7.656	7.836